Designing a Robust Control System Based on Sliding Mode Control for Two-axis Gimbal Systems

Nguyen Viet Phuong
Department of Aerospace Control Systems
Academy of Military Science and Technology
Hanoi, Vietnam
vphuongvtl@gmail.com

Nguyen Duy Khanh
Department of Automatic Control Systems
Saint Petersburg State Electrotechnical University
Hanoi, Vietnam
khanhnguyenmta@gmail.com

Nguyen Trong Tuyen
Department of Biomedical Engineering
Le Quy Don Technical University
Hanoi, Vietnam
nguyentuyen1988@gmail.com

Nguyen Ngoc Hung
Department of Aerospace Control Systems
Le Quy Don Technical University
Hanoi, Vietnam
nguyenngochungtk40@gmail.com

***Abstract*— Two-axis gimbals are used in stabilizing and controlling the aiming of optical systems. The main task is to isolate the angular motion of the payload and the disturbances affecting the optical axis of the camera while maintaining the camera's orientation locked onto the target. Currently, two commonly used gimbal structures are the Yaw-Pitch type and the Roll-Swing type. In this paper, we delve into an in-depth study to develop the full mathematical models for both types, thereby analyzing and evaluating the influence of the cross-channel noise moment effects caused by gimbal imbalance on the stability and aiming control quality under complex angular motion conditions of the payload. Simulation results conducted using MATLAB/SIMULINK with the two-axis gimbal model demonstrate that employing a robust control system significantly reduces the impact of disturbances and enhances the quality of control and stability of the transmission system.**

Keywords*— *two-axis gimbal, inertially stabilized platform, sliding mode control, self-driving transmission, adaptive.

I. Introduction

The stabilization and control system of the optical system, such as cameras or optical sensors, is widely used in both military and civilian applications [1]. The main components of the system include the gimbal system, angle sensors, angular velocity sensors, and control system. Depending on the application, the choice of gimbal structure greatly affects the stability and accuracy of the aim. Typically, there are three types of gimbals used: the three-axis gimbal [2], the Yaw-Pitch two-axis gimbal [3], and the Roll-Swing two-axis gimbal [4]. Among them, the three-axis gimbal offers the best stability [2], but it has a complex structure and is usually used for systems with relatively large spaces. Therefore, in some cases where weight and size are limited, a two-axis gimbal is often used, such as in seeker system [5, 6]. The Yaw-Pitch two-axis gimbal is used in many applications because it can independently control two channels according to the coordinate system [7–10]. This is suitable for tracking objects with two axes on the camera image. On the other hand, the Roll-Swing gimbal is controlled in polar coordinates, so it is necessary to convert the camera coordinate system to the gimbal coordinate system. However, according to [4], the biggest advantage of the Roll-Swing gimbal over the Yaw-Pitch gimbal is the ability to expand the field of view. The choice of gimbal structure also depends on the ability to isolate the movements of the device from the optical axis. Therefore, it is necessary to study the effects of moment noise on the stability and control effectiveness of different types of gimbals. This paper aims to explore the feasibility of using gimbals in seeker system of unmanned aerial vehicles (UAV). Therefore, the focus is on investigating and comparing the influence of moment noise on the two types of two-axis gimbals.

II. Building a Mathematical Model and Control Algorithm for Two-axis Gimbals

A. Mathematical model of the two-axis gimbal system

The Yaw-Pitch two-axis gimbal system is shown in Fig. 1, where it illustrates the two rotational axes: Pitch (P) and Yaw (Y). $X_PY_PZ_P$ and $X_YY_PZ_B$ represent the coordinate system for the pitch axis and yaw axis, respectively.

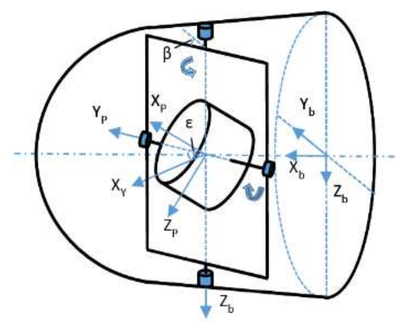

Fig. 1. The structure of the two-axis gimbal system in the yaw-pitch channel.

The angular velocity of the coordinate system along their respective axes is: $\omega^B_{B/I} = [P_b \quad Q_b \quad R_b]^T$, $\omega^P_{P/I} = [p_P \quad q_P \quad r_P]^T$ and $\omega^Y_{Y/I} = [p_Y \quad q_Y \quad r_Y]^T$. Let the inertia matrix of the yaw be denoted as J_Y, and the inertia matrix of the pitch be denoted as J_P.

$$J_Y = \begin{bmatrix} J^Y_x & J^Y_{xy} & J^Y_{xz} \\ J^Y_{xy} & J^Y_y & J^Y_{yz} \\ J^Y_{xz} & J^Y_{yz} & J^Y_z \end{bmatrix}, \; J_P = \begin{bmatrix} J^P_x & J^P_{xy} & J^P_{xz} \\ J^P_{xy} & J^P_y & J^P_{yz} \\ J^P_{xz} & J^P_{yz} & J^P_z \end{bmatrix}$$

We have a dynamic model for the pitch channel [3], as the following.

$$\begin{aligned} J_y^P \dot{q}_P &= T^P + \left(J_z^P - J_x^P\right) p_P r_P + J_{xz}^P \left(p_P^2 - r_P^2\right) \\ &- J_{yz}^P \left(\dot{r}_P - p_P q_P\right) - J_{xy}^P \left(\dot{p}_P + q_P r_P\right) \end{aligned} \quad (1)$$

where T^P represents the total moment acting on the gimbal system, including the moment generated by the motor and the frictional moment. The components containing the inertial moment on the right-hand side of equation (1) represent the cross-coupling relationship when there is motion on other axes.

The equation system, that describes the dynamic model for the yaw channel, as following.

$$J^Y \dot{r}_Y = T_Y + T_{d1} + T_{d2} + T_{d3} \quad (2)$$

$$J^Y = J_z^Y + J_x^P \sin^2 \varepsilon + J_z^P \cos^2 \varepsilon - J_{xz}^P \sin\left(2\varepsilon\right) \quad (3)$$

$$T_{d1} = \left[J_x^Y + J_x^P \cos^2 \varepsilon + J_z^P \sin^2 \varepsilon + J_{xz}^P \sin(2\varepsilon) - \left(J_y^P + J_y^Y\right)\right] p_Y q_Y \quad (4)$$

$$\begin{aligned} T_{d2} &= -\left[J_{xz}^Y + \left(J_z^P - J_x^P\right) \sin\varepsilon \cos\varepsilon + J_{xz}^P \cos(2\varepsilon)\right]\left(\dot{p}_Y - q_Y r_Y\right) \\ &- \left[J_{yz}^P + J_{yz}^P \cos\varepsilon - J_{xy}^P \sin\varepsilon\right]\left(\dot{q}_Y + p_Y r_Y\right) - \left[J_{xy}^Y + J_{xy}^P \cos\varepsilon + J_{yz}^P \sin\varepsilon\right]\left(p_Y^2 - \right. \end{aligned} \quad (5)$$

$$\begin{aligned} T_{d3} &= \ddot{\varepsilon}\left(J_{xy}^P \sin\varepsilon - J_{yz}^P \cos\varepsilon\right) + \dot{\varepsilon}\left[\left(J_{yz}^P \sin\varepsilon + J_{xy}^P \cos\varepsilon\right)\left(q_P + q_Y\right) - J \right. \\ &+ \dot{\varepsilon}\left[\left(J_x^P - J_z^P\right)\left(p_Y \cos 2\varepsilon - r_Y \sin 2\varepsilon\right) + 2J_{xz}^P \left(p_Y \sin 2\varepsilon + r_Y \cos 2\varepsilon\right)\right] \end{aligned} \quad (6)$$

Equation (2) is the differential form of the angular velocity about the z-axis of the yaw of the two-axis gimbal. Here, T_Y represents the total moment acting on this axis. The components T_{d1}, T_{d2}, and T_{d3} are noises caused by the cross-coupling effects between the channels affecting the gimbal system. J^Y, β, and ε are the total moments of inertia about the z-axis, the yaw channel rotation angle about the axis Z_b, and the pitch channel rotation angle about the axis Y_P, respectively. From equations 4–6, it is evident that the disturbances caused by the cross-coupling effects are difficult to completely eliminate through mechanical design.

B. Building the control algorithm

1) Determining the control law for the self-driving transmission system

Sliding Mode Control (SMC) is a suitable choice for the control of the self-driving transmission (SDT) system for several reasons: it can be directly applied to nonlinear systems; it has a short settling time; small tracking error; high robustness; adaptability to parameter uncertainties and disturbances; and it can synthesize controllers for both main loops (stability and position tracking) simultaneously.

2) New proposal for sliding mode control law for self-driving transmission system

In order to increase convergence speed and remedy the vibration factor in sliding mode control (SMC), the work proposes a new approach for the variable *s,* and the parameters $k_1 > 0, k_2 > 0, 0 < r_1 < 1, r_2 > 1$, as follows:

$$\dot{s} = -k_1 \left|s\right|^{r_1} \operatorname{sgn}(s) - k_2 \left|s\right|^{r_2\left(1+\frac{\operatorname{sgn}(|s|-1)}{2}\right)} \operatorname{sgn}(s) \quad (7)$$

The adaptive power reaching law (APRL) is named as such due to its characteristic of automatically adjusting the exponent coefficient based on the value of $\left|s\right|$.

The variables s and $\dot{s}$ in the sliding control law described by equation (7) can converge to the equilibrium point (0,0) after a finite time. The convergence condition is guaranteed according to the Lyapunov stability criterion.

Synthesis of sliding mode control laws for a self-driving transmission system

Let $x_1 = \lambda_y^h$, $x_2 = \dot{\lambda}_y^h = q_P$, $x_3 = \lambda_z^h$, $x_4 = \dot{\lambda}_z^h = r_P$, where λ_y^h, λ_z^h represent the respective inertial angles of the self-driving transmission along the y and z axes. From equation (1) and (2), we have the state-space model for the self-driving transmission system, as follows:

$$\begin{cases} \dot{x}_1 = x_2;\ \dot{x}_2 = f_1\left(x_2, x_4\right) + \dfrac{T_m^P - T_f^P}{J_y^P} + T_D^P; \\ \dot{x}_3 = x_4;\ \dot{x}_4 = f_2\left(x_2, x_4\right) + \dfrac{(T_m^Y - T_f^Y)\cos\varepsilon}{J^Y} + T_D^Y \end{cases} \quad (8)$$

where f_1, f_2, T_D^P, T_D^Y are nonlinear functions representing the cross-coupling between channels from equation (1) and equation (4)–(6). $T_m^P, T_m^Y, T_f^P, T_f^Y$ are the motor torque and friction for each channel.

The angular error and angular velocity error between the desired value and the actual value are:

$$\begin{cases} e_1 = \lambda_y - x_1 \\ \dot{e}_1 = \dot{\lambda}_y - x_2 \end{cases};\ \begin{cases} e_2 = \lambda_z - x_3 \\ \dot{e}_2 = \dot{\lambda}_z - x_4 \end{cases} \quad (9)$$

where, $\lambda_y, \dot{\lambda}_y$, $\lambda_z, \dot{\lambda}_z$ represent the angular position and angular velocity of the aiming direction along the y and z axes.

Applying Fast Terminal Sliding Mode Control (FTSMC) for the sliding surface, we have:

$$\begin{cases} s_1 = \dot{e}_1 + \tau_{11} e_1 + \tau_{12} e_1^{\delta_1} \\ s_2 = \dot{e}_2 + \tau_{21} e_2 + \tau_{22} e_2^{\delta_2} \end{cases} \quad (10)$$

with $\tau_{11}, \tau_{12} > 0$; $\tau_{21}, \tau_{22} > 0$; $0 < \delta_1, \delta_2 < 1$.

Applying the proposed APRL from the formula (7), we have:

$$\begin{cases} \dot{s}_1 = -k_{11} \left|s_1\right|^{r_{11}} \operatorname{sgn}(s_1) - k_{12} \left|s_1\right|^{r_{12}\left(1+\frac{\operatorname{sgn}(|s_1|-1)}{2}\right)} \operatorname{sgn}(s_1) \\ \dot{s}_2 = -k_{21} \left|s_2\right|^{r_{21}} \operatorname{sgn}(s_2) - k_{22} \left|s_2\right|^{r_{22}\left(1+\frac{\operatorname{sgn}(|s_2|-1)}{2}\right)} \operatorname{sgn}(s \end{cases} \quad (11)$$

where $k_{11}, k_{12} > 0$; $k_{21}, k_{22} > 0$; $0 < r_{11}, r_{21} < 1$; $r_{21}, r_{22} > 1$.

Differentiating the equation system (10) and using the system model (8), we have the SMC law for the SDT system:

$$
\begin{cases}
T_m^P = J_y^P\left[\ddot{\lambda}_y - \dot{s}_1 - f_1(x_2,x_4) - T_D^P + \tau_{11}\dot{e}_1 + \tau_{12}\dfrac{d}{dt}e_1^{\delta_1}\right] \\
+\hat{T}_f^P; \\
T_m^Y = \dfrac{J_y^Y}{\cos\varepsilon}\left[\ddot{\lambda}_z - \dot{s}_2 - f_2(x_2,x_4) - T_D^Y + \tau_{21}\dot{e}_2 + \tau_{22}\dfrac{d}{dt}e_2^{\delta_2}\right] \\
+\hat{T}_f^Y.
\end{cases}
\tag{12}
$$

3) Implementing the system and demonstrating its stability

To implement the sliding mode control law (12), the following parameters are required: the angular error, angular velocity, and angular acceleration of the aiming direction; the angles and angular velocities of the SDT axes relative to the UAV body; the inertial angular velocity; the inertial moment of the gimbal channels; and the estimated moment of frictional noise. These pieces of information can be directly measured and estimated using the image processing and tracking system of the target and the sensors mounted on the SDT. The frictional moment can be estimated using a neural network based on a radial basis function (RBF) model. In that case, the frictional moment component is given by:

$$\mathbf{T}_f = \mathrm{W}^T\mathbf{h}(\mathbf{x}) + \boldsymbol{\varepsilon} \tag{13}$$

With the input vector $\mathbf{x} = [x_1 \quad x_2]^T = [r^P \quad q^P]^T$; frictional moment vector $\mathbf{T}_f = [T_f^Y \quad T_f^P]^T$; RBF vector $\mathbf{h} = [h_1 \quad h_2 \quad h_3 \quad h_4 \quad h_5]^T$ and ideal weight matrix $\mathrm{W}=[W_{ij}]^T$; $\boldsymbol{\varepsilon}$ - differential approximation error. In this case, the approximate frictional moment can be calculated by as follows:

$$\hat{\mathbf{T}}_f = \hat{\mathrm{W}}^T\mathbf{h}(\mathbf{x}) \tag{14}$$

Let $\mathbf{e} = [e_1 \quad e_2]^T$ be the vector representing the angular error, $\mathbf{s} = [s_1 \quad s_2]^T$ be the sliding surface vector, $\mathbf{b} = diag(1/J_y^P,\ \cos\varepsilon/J_y^Y), \mathbf{k}_1 = diag(k_{11}, k_{21}), \mathbf{k}_2 = diag(k_{12}, k_{22})$. Then, we select the Lyapunov function as follows:

$$L = 1/2[\mathrm{s}^T\mathbf{s} + tr(\tilde{\mathrm{W}}\Gamma^{-1}\tilde{\mathrm{W}}^T)] \tag{15}$$

In that case, if the adaptive law is chosen for the weight matrix:

$$\dot{\hat{\mathrm{W}}} = -\mathrm{hs}^T\mathbf{b}\Gamma \tag{16}$$

And if the condition $|\mathbf{k}| > |\mathbf{b}\boldsymbol{\varepsilon}_{\max}|$ is satisfied, then we have $\dot{L} < 0$, and we can conclude that the system is stable.

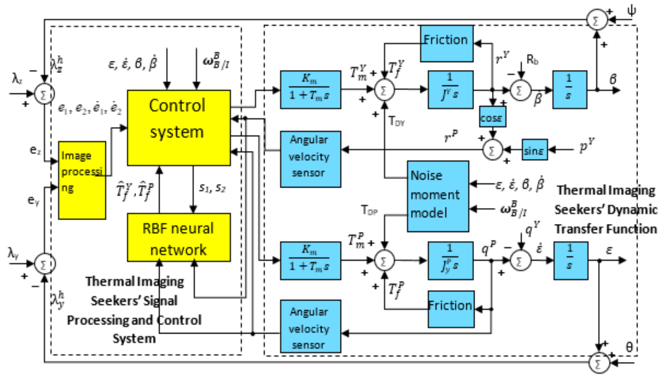

Fig. 2. The structure diagram of the SDT control system

The structure diagram of the SDT control system is shown in Fig. 2. The general task of both control loops for the Yaw and Pitch channels is to track the angle of the self-driving optical axis with the aiming angle and simultaneously eliminate disturbances caused by the rotational motion of the UAV body and friction.

III. SIMULATION RESULTS AND EVALUATION

To evaluate the effectiveness of the control law for the self-driving thermal imaging transmission system using the Yaw-Pitch gimbal proposed in Section II, below are the investigations and assessments of the control law through simulations on Matlab-Simulink.

The initial parameters are: Motor $K_m = 0.85$, $T_m = 0.0135$, Coulomb friction $F_c = 0.03$ (N.m), static friction $F_s = 0.06$ (N.m), viscous friction coefficient $F_v = 0.057$ (N.m/rad/s), Stribeck velocity $v_s = 0.05$ (rad/s), inertial moment (Kg.m^2):

$$J^Y = \begin{bmatrix} 0.0054 & -0.003 & -0.002 \\ -0.003 & 0.0025 & -0.003 \\ -0.002 & -0.003 & 0.0032 \end{bmatrix},, J^P = \begin{bmatrix} 0.0024 & -0.001 & -0.0005 \\ -0.001 & 0.0012 & -0.001 \\ -0.0005 & -0.001 & 0.0018 \end{bmatrix}$$

In this research, we proposed two simulation scenarios for the SDT system, which are listed in Table I.

TABLE I THE SIMULATION SCENARIOS FOR SDT SYSTEM.

Scenarios	Angular velocity of the UAV body $\omega_{B/I}^B$ (deg/s)			Target motion		Friction
	P_b	Q_b	R_b	*Yaw channel*	*Pitch channel*	
1	0	0	0	Sine	Pulse	Excluding
2	60sin(ωt)	60sin(ωt)	60sin(ωt)	Sine	Pulse	Including

Typical control laws such as PID, SMC (Sliding Mode Control) based on the Exponential Reaching Law (ERL) are selected for comparison with the newly proposed APRL.

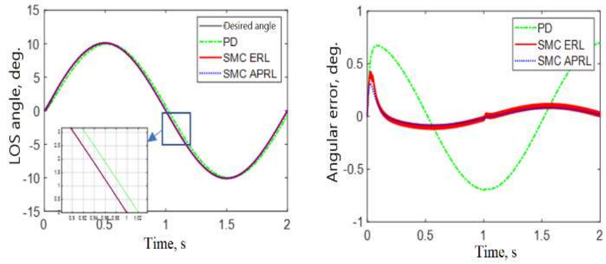

Fig. 3. The simulation results of the yaw channel of the SDT system according to scenarios 1 (Line of Sight, LOS).

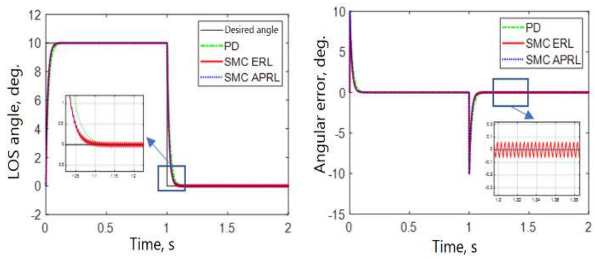

Fig. 4. The simulation results of the pitch channel of the transmission system according to scenarios 1.

In scenario 1 (Fig. 3 and Fig. 4), when there are no disturbances affecting the system, all three control laws, including PID, sliding mode control (SMC) based on the exponential reaching law (ERL), and the proposed adaptive power reaching law (APRL), demonstrate relatively good performance. This is characterized by fast response times and small tracking errors. However, the ERL control law exhibits oscillations around the value of 0 in some cases.

In scenario 2 (Fig. 5 and Fig. 6), when there are disturbances caused by the UAV body's rotation and frictional moments, the tracking errors of all control laws increase. Among them, the PID controller is most affected by the largest tracking error, while the proposed controller is less affected than the other two controllers and still ensures relatively small tracking errors.

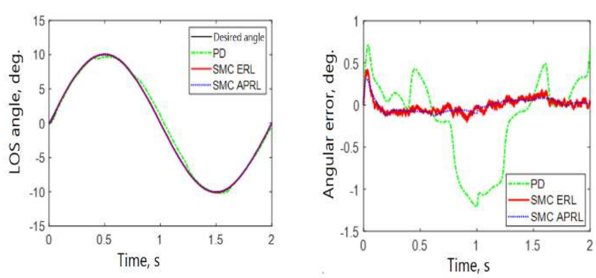

Fig. 5. The simulation results of the yaw channel of the SDT system according to scenarios 2.

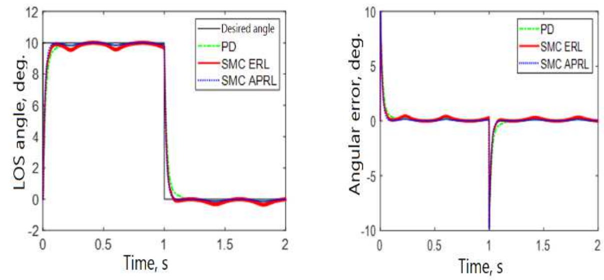

Fig. 6. The simulation results of the pitch channel of the transmission system according to scenarios 2.

IV. Conclusion

In this article, the focus has been on analyzing solutions to the problem of controlling and stabilizing the aiming system applied in the seeker system. The study involved constructing a mathematical model of the typical two-axis gimbal, namely the Yaw-Pitch, and also investigating the influence of cross-coupling on the gimbal systems. The paper conducted simulations to examine several typical cases as a basis for evaluating and comparing the effects of moment disturbances on the stability and control of different types of gimbals. Based on the study of the SMC law and the analysis of its strengths and weaknesses, the paper presented a new approach law (APRL) aimed at improving the convergence time of state variables and reducing vibration issues.

References

[1] J. Hilkert, “Inertially stabilized platform technology concepts and principles,” IEEE control systems magazine, Vol. 28(1), pp. 26-46, 2008.

[2] A. Altan, R. Hacioğlu, “Modeling of three-axis gimbal system on unmanned air vehicle (UAV) under external disturbances,” 2017 25th Signal Processing and Communications Applications Conference (SIU), pp. 1-4, 2017.

[3] B. Ekstrand, “Equations of motion for a two-axes gimbal system,” IEEE Transactions on Aerospace and Electronic Systems, Vol. **37**(3).pp. 1083-1091, 2001.

[4] Y. Bai et al., “Design and analysis of Roll-Swing imaging seeker scan scheme,” 2010 The 2nd International Conference on Industrial Mechatronics and Automation, pp. 100-104, 2010.

[5] H. Jiang, H. Jia, Q. Wei, “Analysis of zenith pass problem and tracking strategy design for roll–pitch seeker,” Aerospace Science and Technology, Vol.. **23**(1), pp. 345-351, 2012.

[6] X. Z. Mu, S. P. Zhou, and G. J. Zhao, “Analysis and evaluation of new approach of AIM-9X AAM seeker,” Infrared and Laser Engineering, Vol. **35**(4): p. 392, 2006.

[7] M. M. Abdo, et al., “Stabilization loop of a two axes gimbal system using self-tuning PID type fuzzy controller,” ISA transactions, Vol. **53**(2), pp. 591-602, 2014

[8] J. Bharali, M. Buragohain, “Design and performance analysis of fuzzy LQR; fuzzy PID and LQR controller for active suspension system using 3 degree of freedom quarter car model,” 2016 IEEE 1st International Conference on Power Electronics, Intelligent Control and Energy Systems (ICPEICES), pp. 1-6, 2016.

[9] N. Ghaeminezhad, W. Daobo, F. Farooq, “Stabilizing a gimbal platform using self-tuning fuzzy PID controller,” International Journal of Computer Applications, Vol. **93**(16), 2014.

[10] K. J. Seong, et al., “The stabilization loop design for a two-axis gimbal system using LQG/LTR controller,” 2006 SICE-ICASE International Joint Conference, pp. 755-759, 2006.